AD

④

AD-A191 683

TECHNICAL REPORT BRL-TR-2882

(Supersedes IMR-885)

AERODYNAMIC CHARACTERISTICS OF FIN- AND FLARE-STABILIZED 25 mm XM910 PROTOTYPES

ILMARS CELMINS

December 1987

US ARMY BALLISTIC RESEARCH LABORATORY
ABERDEEN PROVING GROUND, MARYLAND

8 8

DESTRUCTION NOTICE

Destroy this report when it is no longer needed. DO NOT return it to the originator.

The findings of this report are not to be construed as an official Department of the Army position, unless so designated by other authorized documents.

The use of trade names or manufacturers' names in this report does not constitute indorsement of any commercial product.

AD-A191683

REPORT DOCUMENTATION PAGE

1a. REPORT SECURITY CLASSIFICATION	1b. RESTRICTIVE MARKINGS
UNCLASSIFIED	

2a. SECURITY CLASSIFICATION AUTHORITY	3. DISTRIBUTION/AVAILABILITY OF REPORT
2b. DECLASSIFICATION/DOWNGRADING SCHEDULE	

4. PERFORMING ORGANIZATION REPORT NUMBER(S)	5. MONITORING ORGANIZATION REPORT NUMBER(S)
BRL-TR-2882	

6a. NAME OF PERFORMING ORGANIZATION	6b. OFFICE SYMBOL (If applicable)	7a. NAME OF MONITORING ORGANIZATION
U.S. Army Ballistic Research Laboratory	SLCBR-LF	

6c. ADDRESS (City, State, and ZIP Code)	7b. ADDRESS (City, State, and ZIP Code)
Aberdeen Proving Ground, MD 21005-5066	

8a. NAME OF FUNDING/SPONSORING ORGANIZATION U.S. Army Ballistic Research Laboratory	8b. OFFICE SYMBOL (If applicable)	9. PROCUREMENT INSTRUMENT IDENTIFICATION NUMBER
	SLCBR-DD-T	

8c. ADDRESS (City, State, and ZIP Code)	10. SOURCE OF FUNDING NUMBERS			
	PROGRAM ELEMENT NO.	PROJECT NO.	TASK NO.	WORK UNIT ACCESSION NO
Aberdeen Proving Ground, MD 21005-5066	RDT&E	1L162618	AH80	

11. TITLE (Include Security Classification)

AERODYNAMIC CHARACTERISTICS OF FIN- AND FLARE-STABILIZED 25 MM XM910 PROTOTYPES

12. PERSONAL AUTHOR(S)

Celmins, Ilmars

13a. TYPE OF REPORT	13b. TIME COVERED	14. DATE OF REPORT (Year, Month, Day)	15. PAGE COUNT
Final	FROM _____ TO _____		

16. SUPPLEMENTARY NOTATION

This report supersedes IMR-885, dated 19 March 1987

17. COSATI CODES			18. SUBJECT TERMS (Continue on reverse if necessary and identify by block number)
FIELD	GROUP	SUB-GROUP	XM910 Training Round Fin-Stabilized
01	01		25 mm Flare-Stabilized
19	04		

19. ABSTRACT (Continue on reverse if necessary and identify by block number) (ic/ngr)

Test firings of prototype fin- and flare-stabilized 25 mm training rounds were conducted. The fin-stabilized rounds were found to be capable of fulfilling all of the training round ballistic requirements. The flare-stabilized rounds were studied as a possible lower cost alternative. Initially, a large angle flare design, similar to existing tank gun training rounds, was tested, but data showed the configuration drag coefficient was too high. Subsequent computer predictions indicated that a small angle flare would have significantly lower drag and sufficient stability for flight. A four-degree flare was fabricated and fired, confirming the drag and stability predictions.

20. DISTRIBUTION/AVAILABILITY OF ABSTRACT	21. ABSTRACT SECURITY CLASSIFICATION
☐ UNCLASSIFIED/UNLIMITED ☐ SAME AS RPT ☐ DTIC USERS	

22a. NAME OF RESPONSIBLE INDIVIDUAL	22b. TELEPHONE (Include Area Code)	22c. OFFICE SYMBOL
Ilmars Celmins	301-278-4362	SLCBR-LF-F

DD FORM 1473, 84 MAR   83 APR edition may be used until exhausted   SECURITY CLASSIFICATION OF THIS PAGE
All other editions are obsolete

TABLE OF CONTENTS

iii

LIST OF FIGURES

LIST OF FIGURES (Continued)

I. INTRODUCTION

The Army is in the process of developing the XM910 training round to simulate the 25 mm XM919 APFSDS service projectile. BRL is responsible for providing data in support of this program. In order to insure a proper ballistic match to the service round, it is necessary to acquire data on the flight performance of the training round. This report presents the results of aerodynamic studies of a group of XM910 candidate configurations.

The primary training round ballistic requirements are:

1. Less than 1 milliradian center of impact difference from the XM919 over the range of 1000 to 2000 meters.

2. Dispersion within 10 percent of the XM919 dispersion.

3. A maximum range of less than 8000 meters.

An additional requirement is to have a visible trace to 2000 meters. It is also very important to keep the unit cost to a minimum because training rounds are expended in large quantities.

Since the XM919 is a long-rod projectile, it is expected that the best training round configuration for matching both gravity drop and jump would also be a long rod. The simplest long rod training round design is a copy of the XM919 using a lighter weight fin-stabilized rod launched by the same sabots. A lower cost alternative is to use a flare-stabilized rod and thus eliminate the high precision fins, but then the similarity of flight characteristics is more questionable.

This report presents the measured aerodynamic coefficients of three long rod projectile configurations: fin-stabilized; a standard flare; and a new shallow flare. Additionally, Appendix A describes the predictive methods used to estimate the aerodynamic characteristics of the flare-stabilized prototypes and compares the predicted and measured coefficients.

II. TEST PROCEDURE

All tests were conducted in the BRL Aerodynamics Range.[1] The range data were fitted to solutions of the linearized equations of motion and these results used to infer linearized aerodynamic coefficients, using the methods of Reference 2. Various propellants and charge weights were selected to achieve the required test Mach numbers. All rounds were fired from a Mann barrel having the same internal geometry as the M242 cannon. Figure 1 is a photograph of the three training round prototypes, along with an XM881 APFSDS projectile (a forerunner of the XM919). The sabots used for the test program were from a lot originally intended for XM881 projectiles. These sabots incorporate a slip band obturator, which is designed to keep the projectile roll rate below 15 percent of full spin.

Testing was conducted in three stages. The fin-stabilized configuration, XM910 FS, was test fired first. Figure 2 gives the dimensions and physical properties of this projectile. The fins are identical to those of the

1

XM881. The training round rod has the same basic shape as the XM881 rod, but it is slightly shorter and made of steel instead of tungsten, so that it has a much lower ballistic coefficient. A total of twelve rounds were fired - three at the design velocity of 1600 m/s and the rest at lower speeds to get aerodynamic data over a Mach number range of 0.5 to 4.5.

The first flare-stabilized configuration, XM910 CS-V1, was tested next. The design of this round, shown in Figure 3, was loosely based on existing flare-stabilized tank gun training round designs.[3] The flare has a length of 2.67 calibers (rod diameters), and a nominal half-angle of 15 degrees. It is made of aluminum and the inside is hollow in order to keep the total round center of gravity as far forward as possible. The rod used is exactly the same as the rod of the fin-stabilized version. A total of twelve rounds were fired at a total of five different Mach numbers.

A trajectory analysis of this first flare-stabilized configuration, using the measured drag and a muzzle velocity of 1600 meters per second, showed that the maximum range was less than 2000 meters. The obvious conclusion was that a much lower drag coefficient would be needed in order to achieve the required trajectory match. An analysis was then done of the correlation of flare geometry changes to changes in drag coefficient. The details of this analysis are contained in Appendix A. The basic finding was that by using a small flare angle, it was theoretically possible to make a stable, flare-stabilized rod with low enough drag to match the XM919 trajectory.

A new flare-stabilized configuration, XM910 CS-V2, shown in Figure 4, was then tested. The rod shape was again left unchanged and the flare design of this projectile was derived from the previously mentioned analysis. The flare length is 4.5 calibers, and the half-angle is 4 degrees. A salient feature of this design is the similarity of the flare to the fin assembly it replaces. This can readily be seen by comparing the physical properties of the XM910 CS-V2 with those of the XM910 FS projectile.

III. RESULTS

The results will be presented in two parts: first, the drag data and resultant trajectory predictions; and second, the other aerodynamic coefficients. The drag results are emphasized because of their immediate relevance to the training round ballistic requirements: the predicted trajectory match is based on the drag data. The other coefficients are then used to determine static stability and to estimate the relative aerodynamic jump sensitivity of the three configurations.

1. DRAG

The measured drag coefficients for each of the three round types are shown in Figure 5. The actual measured values are given in Tables 1 through 3. The resultant trajectory predictions will be discussed separately for each prototype.

The XM910 FS training round is designed to match the XM919 when fired with a muzzle velocity of 1600 m/s. The measured drag coefficient, Figure 5, was used to compare the predicted trajectory of this round with the XM919

2

trajectory, and the resultant trajectory comparison is shown in Figure 6. The y-axis of this plot is height in meters and the x-axis is downrange distance, also in meters. The quadrant elevation is set for the XM919 trajectory at 2000 meters. Both rounds are "fired" with this same quadrant elevation and the predicted trajectories are plotted, along with the +/- 1 milliradian limits. The maximum trajectory mismatch of -0.41 milliradians occurs at 2000 meters, and the maximum range of this round was predicted to be 7116 meters. Thus, the XM910 FS projectile fulfills all of the training round ballistic requirements.

The drag for the XM910 CS-V1 standard flare was much higher, as shown in Figure 5. A trajectory comparison with the XM919 is shown in Figure 7, using a muzzle velocity of 1600 m/s. The drag is so high that the round falls below the 1 milliradian limit at approximately 700 meters, and the maximum range is only 1760 meters.

The XM910 CS-V2 drag is much closer to that of the fin-stabilized round. The trajectory of this shallow flare projectile is compared with the XM919 in Figure 8, again using a muzzle velocity of 1600 m/s. Since the predicted trajectory mismatch at 2000 meters is -1.93 milliradians, this round does not meet the training round ballistic requirements. However, the improvement over the CS-V1 performance is significant.

All of the measured drag data was for rounds without tracers. Since a visible trace is one of the training round requirements, the expected effect of a tracer on the drag needs to be examined. This effect would be minimal for the fin-stabilized configuration because of the small base area and proportionately low base drag. Although the tracer effect would be much larger for the 15-degree flare, the total drag of this round is so large that even if the base drag were completely eliminated, the drag would still be too high for the training round ballistic requirements.

This is not the case, however, for the XM910 CS-V2 shallow-angle flare. At high Mach numbers, approximately half of the total drag is base pressure drag for this configuration. Recent tests of 25 mm spin-stabilized projectiles showed that a high mass flow tracer was capable of reducing the base drag by up to 50%. If such a tracer could be put in the hollow flare cavity, a similar base drag reduction should occur. Figure 9 shows the predicted effect on the drag curve of such a tracer. This plot includes the non-traced drag, the predicted traced drag, and the fin-stabilized drag for comparison. The sharp rise in drag at Mach 2 is due to tracer burnout, and helps to limit the maximum range of the round. The magnitude of the drag coefficient during trace burn is very close to that measured for the fin-stabilized projectile. Figure 10 shows a trajectory comparison to the XM919 using this predicted drag. The maximum mismatch is +0.19 milliradians and the maximum range is 6350 meters. Figure 11 illustrates the maximum range characteristics of all of the XM910 configurations. For this plot, each round is "fired" at the quadrant elevation that will yield maximum range for that round. The predicted trajectories are shown, indicating that the maximum range requirement will not be a problem for any of the configurations.

2. AERODYNAMIC PERFORMANCE

The measured aerodynamic coefficients are: static moment coefficient,

3

lift coefficient, pitch damping moment coefficient, Magnus moment coefficient and static margin. The measured values are given in Tables 1 through 3, and each coefficient is discussed in detail in the following paragraphs. The tables contain all of the data that was obtained, although the accuracy with which some of the coefficients were determined is marginal. The plots of the coefficients include curves that are judged to be a best estimate of the data trends, based on past experience. There is a significant amount of scatter in the data, most of which is due to variations in yaw levels for individual shots. The plotted coefficients are not corrected for yaw effects because there were not enough data points to make this correction.

The static moment coefficient as a function of Mach number is presented in Figure 12. For static stability, it is desirable that this coefficient have a large negative value. At the launch Mach number of 4.5, the 15-degree flare has the largest negative value, followed by the fin, with the 4-degree flare having the smallest. An interesting aspect of the plot is that the static moment coefficient remains relatively constant with Mach number for the flares, but shows a large variation for the fin-stabilized prototype. This difference in the data trends is indicative of the fact that flares and fins are not aerodynamically alike. This may or may not be a problem when trying to match the trajectory of a fin-stabilized round with a flare-stabilized training round.

The data for the lift coefficient, Figure 13, are similar to that of the static moment coefficient. The 4-degree flare has the lowest lift coefficient, the 15-degree flare has the highest, and at launch, the fin-stabilized design falls between the two. Additionally, the trend is the same as for the static moment coefficient, i.e., going from a 4-degree flare to 15 degrees increases the lift coefficient. A high lift coefficient is not necessarily desirable, but is usually required in order to get a large negative static moment coefficient.

The static margin is essentially a ratio of the moment coefficient over the lift coefficient, so the trends mimic those of its component parts, Figure 14. A round is usually considered to be statically stable if the static margin is greater than 0.5 (Appendix A). The three configurations tested are statically stable at all Mach numbers, and, at launch, the 15-degree flare is the most stable.

The pitch damping moment coefficient variation with Mach number is given in Figure 15. Here the trends are different. The 4-degree flare design has the smallest values of pitch damping, followed by the 15-degree flare values, with the fin-stabilized design having the best pitch damping characteristics. Rough estimates of the variation of pitch damping with yaw indicate that the pitch damping moment coefficient at launch Mach numbers is approximately -150 for the 4-degree flare, -200 for the 15-degree flare, and -350 for the fin-stabilized design.

The Magnus moment characteristics of the three configurations are plotted in Figure 16. Roll data were not taken for any configuration tested, so the given values are based on the roll history deduced from the yaw reduction. The fin-stabilized design has a strong negative Magnus moment coefficient, whereas both of the flare-stabilized configurations have coefficients of lower absolute value. Variations of Magnus with yaw indicate that, for low yaw,

4

both of the flare-stabilized designs have Magnus moment coefficients close to zero. This is because a flare is a compression surface, which tends to retard boundary layer growth on the flare portion of the projectile. The fin-stabilized design exhibits the apparent Magnus moment caused by rolling fins.[4] It is desirable to have a Magnus moment coefficient with a low absolute value, and all three of the training round prototypes fulfill this criterion.

IV. CONCLUSIONS

Of the three configurations tested, only the fin-stabilized version fulfills the training round ballistic requirements. The 15-degree flare was found to have ample stability, but the drag was too high. The 4-degree flare reduced drag significantly, but still did not meet the ballistic requirements in the untraced configuration. However, predictions have shown that the addition of a high mass flow tracer to this round would provide sufficient drag reduction for an excellent trajectory match with the XM919, while fulfilling the maximum range requirement.

Although the 4-degree flare was shown to be stable in flight, some of the measured aerodynamic coefficients were found to be significantly different from those of the fin-stabilized training round version, which is assumed to be aerodynamically similar to the service round. However, the data indicate that, if required, a flare-stabilized round can be designed having similar aerodynamic characteristics to those of a fin-stabilized design at launch conditions. A configuration that is suggested by the measured data would have a flare angle somewhere between 4 and 15 degrees and a flare length between 2.7 and 4.5 calibers. At launch, such a design would have a static moment coefficient, lift coefficient, and static margin very close to those of the fin-stabilized design. However, this "moderate flare" would still have a lower pitch damping moment coefficient than the finner. To first order, this means that the moderate flare, when compared to the fin-stabilized design, should have the same yaw frequency and aerodynamic jump sensitivity. The low pitch damping, however, would result in a slower yaw decay with downrange distance.

The implication of these results is that both the drag and aerodynamic performance requirements of the training round can be met with flare-stabilized designs. It is not clear, however, that both the drag and performance goals can be achieved by the same configuration. The 4-degree XM910 CS-V2 comes close, but has some differences in aerodynamic coefficients. The significance of these differences in terms of jump and dispersion must be determined by test firings.

V. RECOMMENDATIONS

The concept of using a small-angle flare as a stabilization mechanism should be investigated further. Testing needs to be done in order to determine the dispersion characteristics of the round as well as the actual effect of a high mass flow tracer on drag.

If a larger static margin is required in order to compensate for the

additional weight of the tracer and/or to reduce dispersion, then other flare configurations will need to be examined. It may be possible to use a biconic flare to get the desired balance between drag and stability.

There is no apparent reason that a small-angle flare cannot be used on larger caliber (i.e. tank gun) training rounds as well. Since aerodynamic coefficients are dimensionless, the results of this report should be directly applicable to a larger round with the same aerodynamic shape, with no more than minor adjustments for Reynolds number effects.

TABLE 1. Aerodynamic Coefficients of the XM910 FS Projectile.

ROUND NUMBER	MACH NUMBER	AVERAGE YAW (deg.)	DRAG COEFFICIENT C_D	STATIC MOMENT COEFFICIENT C_{M_α}	LIFT COEFFICIENT C_{L_α}	STATIC MARGIN ΔX_{CP}	PITCH DAMPING COEFFICIENT $(C_{M_q} + C_{M_{\dot\alpha}})$	MAGNUS MOMENT COEFFICIENT $C_{M_{p\alpha}}$
17584	4.92	7.91	0.52	-18.72	9.64	1.65	-428.8	-56.6
17583	4.89	0.54	0.26	-19.66	12.79	1.51	-383.2	6.2
17579	4.56	1.00	0.29	-23.36	9.97	2.28	-65.2	-7.7
17596	2.82	0.54	0.48	-34.99	6.58	4.96	-545.8	-11.7
17585	2.78	1.86	0.51	-32.83	8.66	3.58	-569.7	-40.7
17586	2.78	6.18	0.64	-32.38	11.00	2.79	-620.6	-58.1
17587	1.38	4.61	1.11	-55.92	12.91	3.99	-742.8	-30.3
17588	1.34	1.21	0.77	-50.99	15.14	3.21	-684.3	-18.1
17589	0.92	1.52	0.74	-58.40	15.76	3.54	-612.6	-41.0
17590	0.91	1.49	0.69	-57.69	12.07	4.52	-697.1	-47.7
17592	0.75	2.50	0.70	-54.29	11.79	4.35	-79.1	-24.2
17591	0.67	2.54	0.64	-51.50	12.05	4.06	-585.2	-53.8

TABLE 2. Aerodynamic Coefficients of the XM910 CS-VI Projectile.

ROUND NUMBER	MACH NUMBER	AVERAGE YAW (deg.)	DRAG COEFFICIENT C_D	STATIC MOMENT COEFFICIENT C_{M_α}	LIFT COEFFICIENT C_{L_α}	STATIC MARGIN ΔX_{CP}	PITCH DAMPING COEFFICIENT $(C_{M_q} + C_{M_{\dot\alpha}})$	MAGNUS MOMENT COEFFICIENT $C_{M_{p\alpha}}$
17872	4.51	3.42	1.46	-35.71	12.22	2.61	-377.2	-5.5
17871	4.49	0.39	1.42	-43.92	11.69	3.35	-194.9	-3.4
17870	4.41	0.42	1.46	-39.59	17.87	2.05	-27.6	1.7
17874	3.14	4.63	2.03	-29.74	9.75	2.52	-318.1	0.7
17873	3.01	2.20	2.06	-32.49	9.55	2.80	-360.8	-20.8
17875	2.96	1.90	2.07	-31.79	9.45	2.76	-435.1	-15.4
17877	1.27	2.36	5.80	-53.62	11.38	3.12	-254.4	-15.8
17878	1.21	6.34	4.63	-40.49	7.42	3.36	-419.7	-5.9
17880	0.87	7.36	3.13	-37.45	8.82	3.13	-430.0	-2.5
17879	0.81	6.95	2.91	-36.85	8.65	3.13	-427.1	-0.9
17881	0.65	2.14	2.43	-43.89	11.03	3.26	-269.2	-21.0
17682	0.65	4.11	2.53	-39.02	10.22	3.06	-325.6	-12.1

8

TABLE 3. Aerodynamic Coefficients of the XM910 CS-V2 Projectile.

ROUND NUMBER	MACH NUMBER	AVERAGE YAW (deg.)	DRAG COEFFICIENT C_D	STATIC MOMENT COEFFICIENT C_{M_α}	LIFT COEFFICIENT C_{L_α}	STATIC MARGIN ΔX_{cf}	PITCH DAMPING COEFFICIENT $(C_{M_q} + C_{M_{\dot\alpha}})$	MAGNUS MOMENT COEFFICIENT $C_{M_{p\alpha}}$
17908	4.56	2.20	0.40	-2.99	5.16	0.51	-215.0	5.0
17907	4.59	1.82	0.42	-3.63	5.37	0.64	-253.0	-0.1
17906	4.56	--	0.38	--	--	--	--	--
17911	4.53	0.92	0.40	-5.57	5.41	0.93	-176.5	-7.0
17986	4.51	4.85	0.45	-4.15	5.68	0.66	-375.5	13.0
17909	3.10	3.89	0.66	-3.87	6.00	0.54	-588.6	16.1
17910	2.92	0.57	0.62	-4.00	5.15	0.67	-300.0	1.6
17980	2.29	7.49	1.03	-5.29	4.84	0.94	-597.1	31.7
17987	2.26	2.28	0.81	-4.99	5.39	0.82	-341.6	-0.6
17914	1.82	0.45	1.09	-13.60	4.98	2.21	-121.6	-5.1
17915	1.80	3.50	1.21	-10.52	5.42	1.60	-413.4	4.7
17913	0.99	4.81	1.14	-16.41	5.89	2.35	-420.0	4.3
17917	0.83	2.85	0.91	-18.24	5.54	2.78	-253.8	-12.0
17923	0.82	1.37	0.90	-23.39	6.75	3.07	-481.7	-34.8
17919	0.79	5.50	1.13	-14.76	5.92	2.07	-442.5	10.7

9
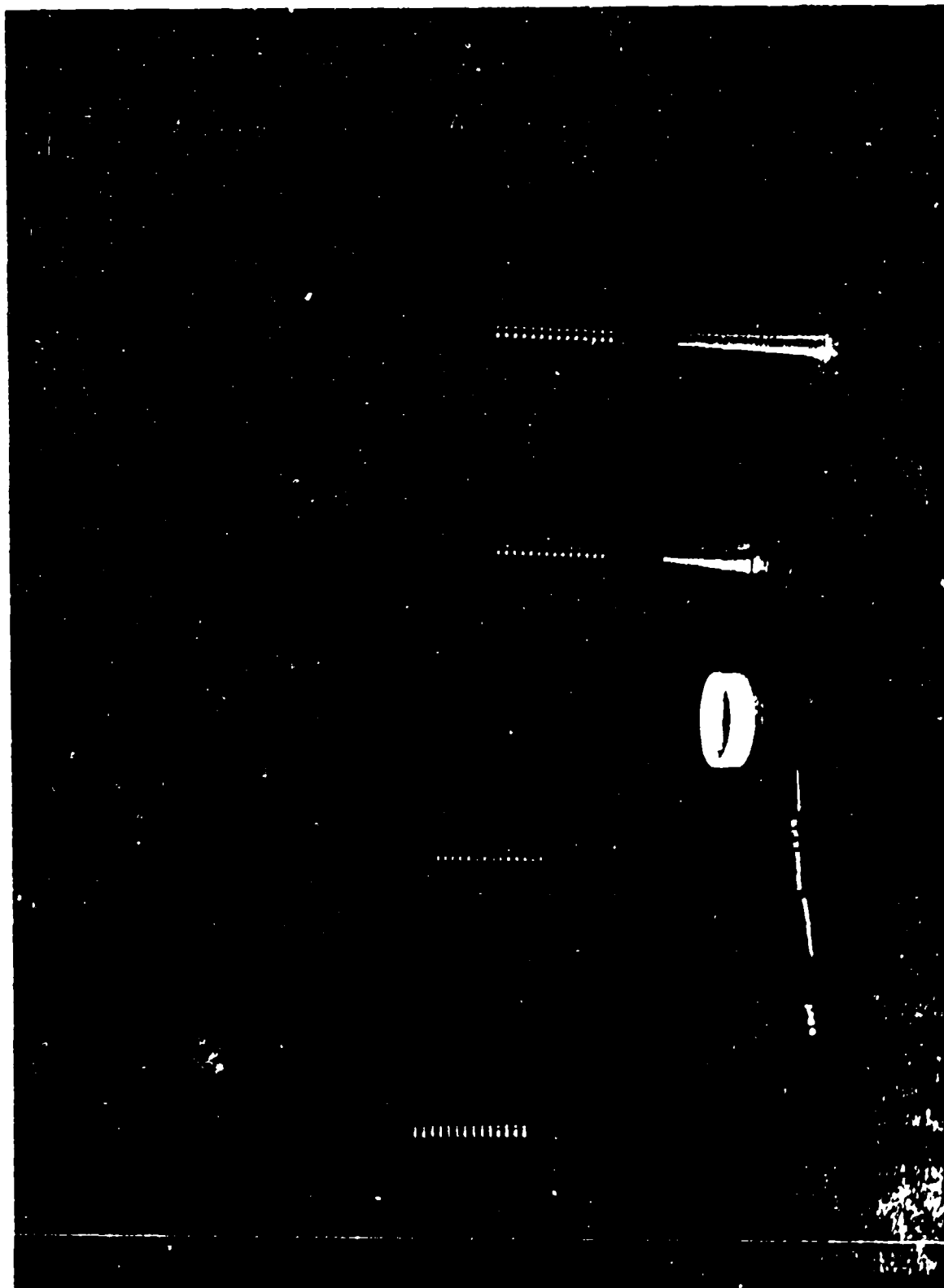
Figure 1. Photograph of (left to right) XM881, XM910 FS, XM910 CS-V1, and XM910 CS-V2.

10
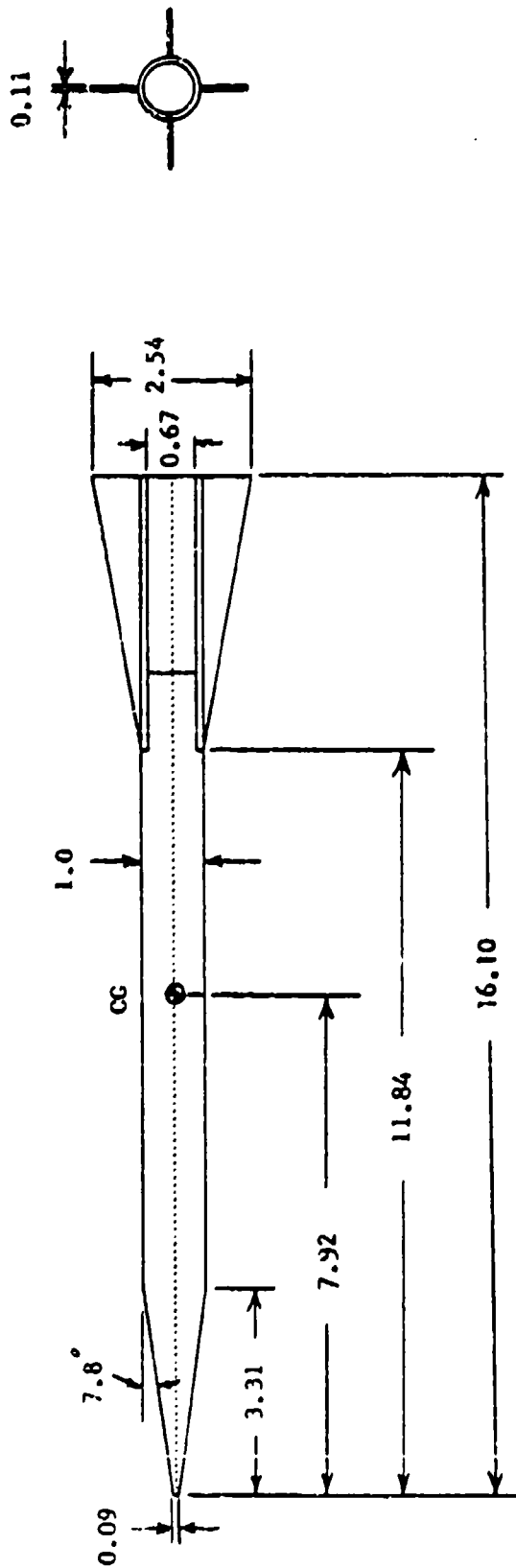
ALL DIMENSIONS IN CALIBERS

(1 CALIBER = 0.83 cm)

WT = 37.7 gm

I_x = 3.20 gm-cm^2

I_y = 346 gm-cm^2

Figure 2. XM610 FS projectile, dimensions and physical properties.

11
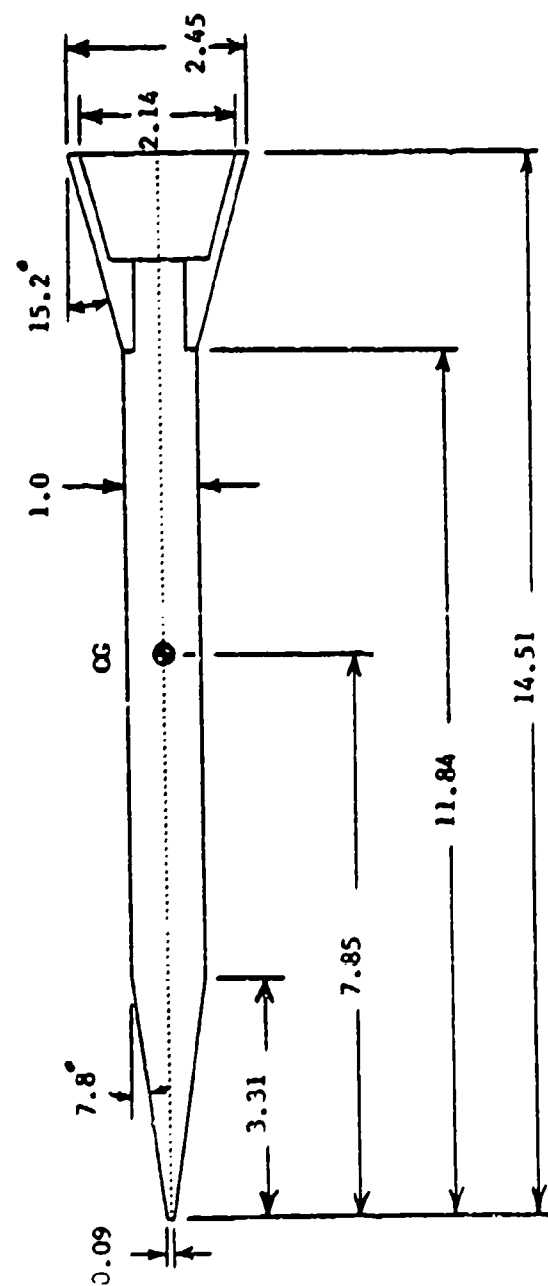
ALL DIMENSIONS IN CALIBERS

(1 CALIBER = 0.83 CM)

WT = 37.9 gm

I_x = 4.37 gm-cm^2

I_y = 324 gm-cm^2

Figure 3. XM910 CS-V1 projectile, dimensions and physical properties.
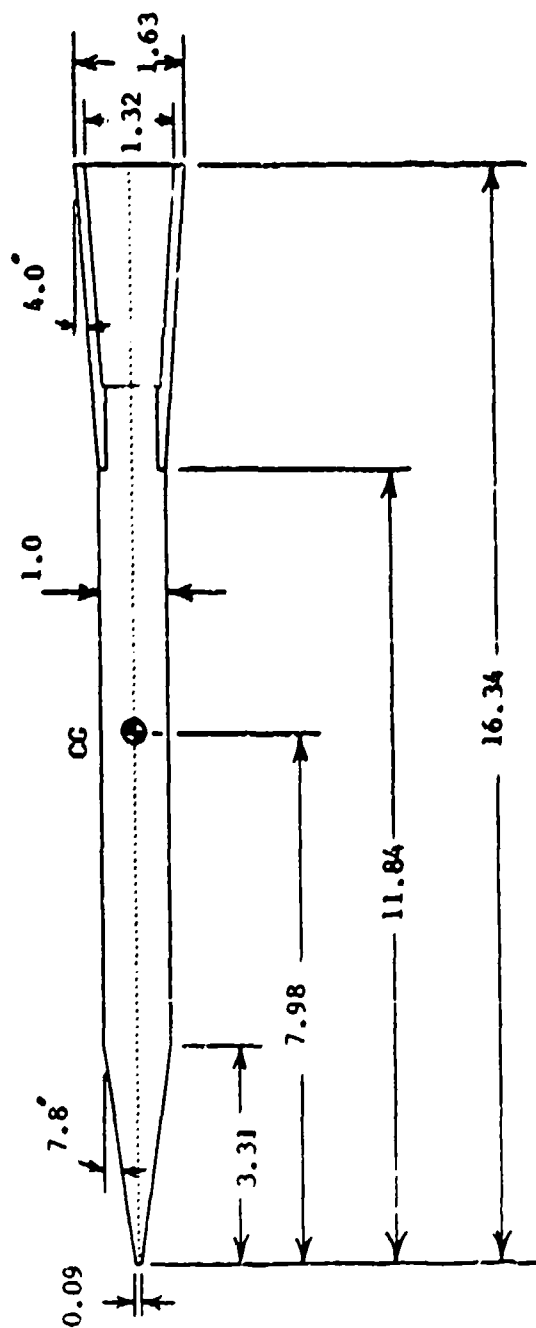
Figure 4. XM910 CS-V2 projectile, dimensions and physical properties.
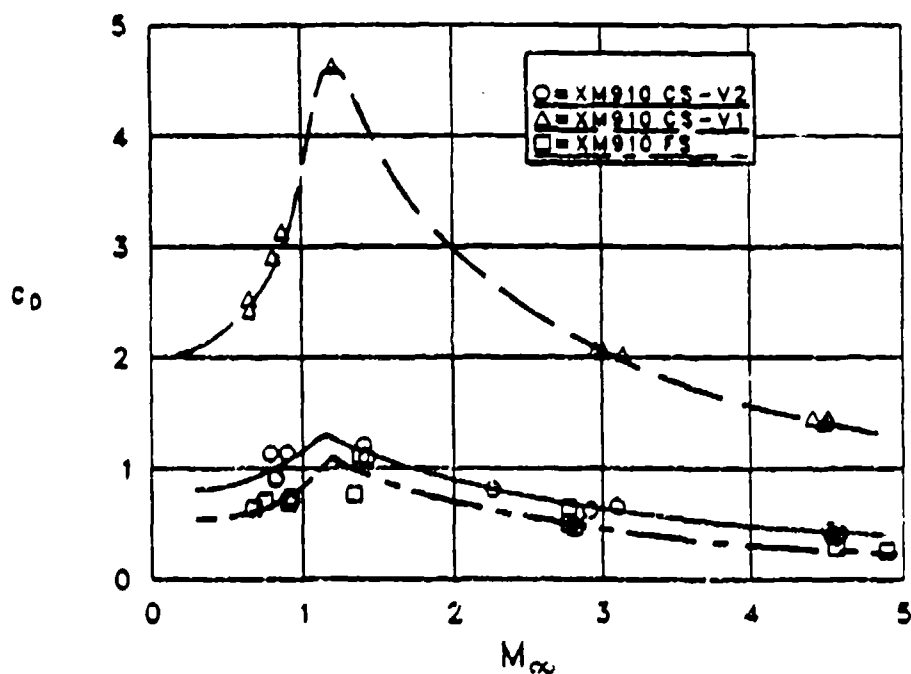
Figure 5. Coefficient of drag versus Mach number.
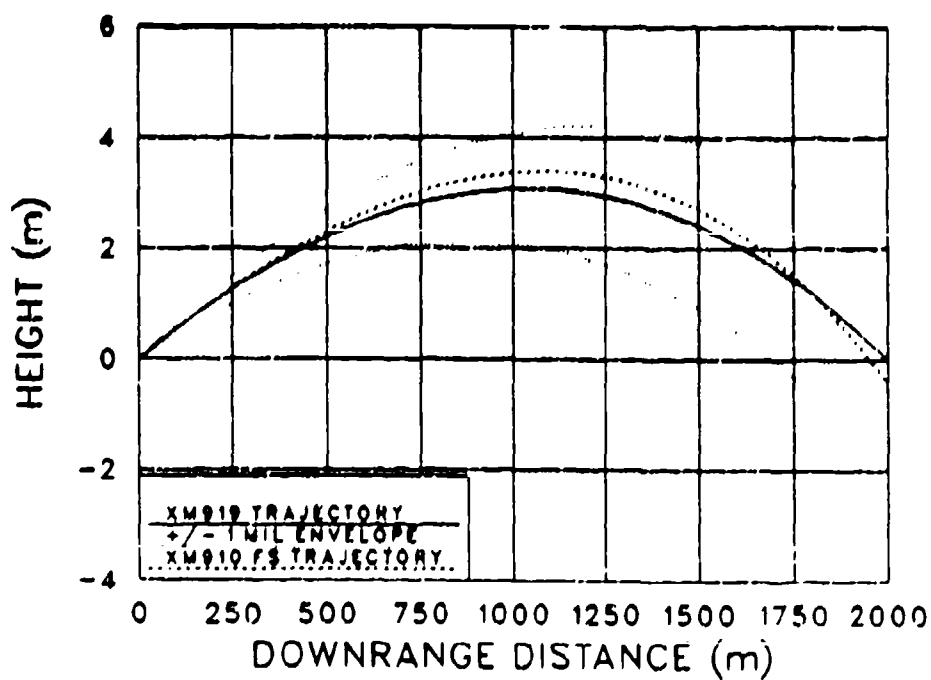
Figure 6. Trajectory comparison of XM910 FS with XM919.

14
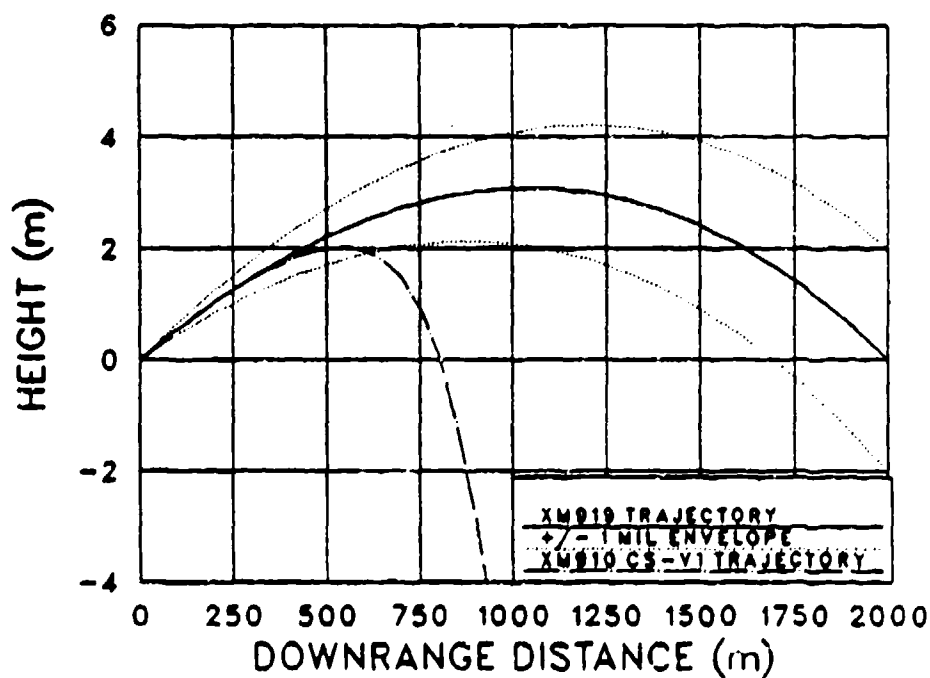
Figure 7. Trajectory comparison of XM910 CS-V1 with XM919.
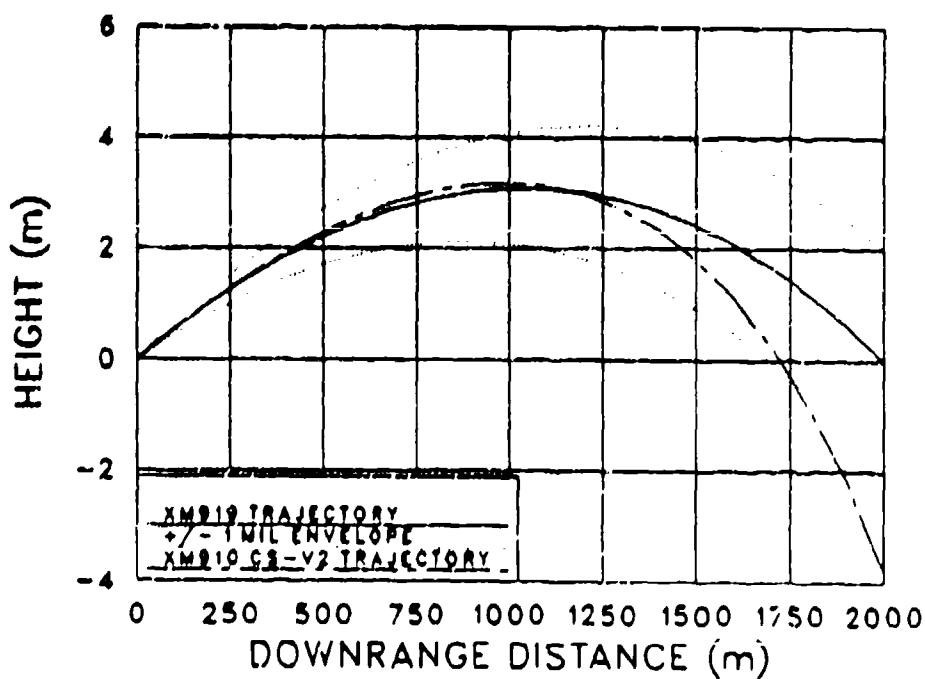
Figure 8. Trajectory comparison of XM910 CS-V2 with XM919.
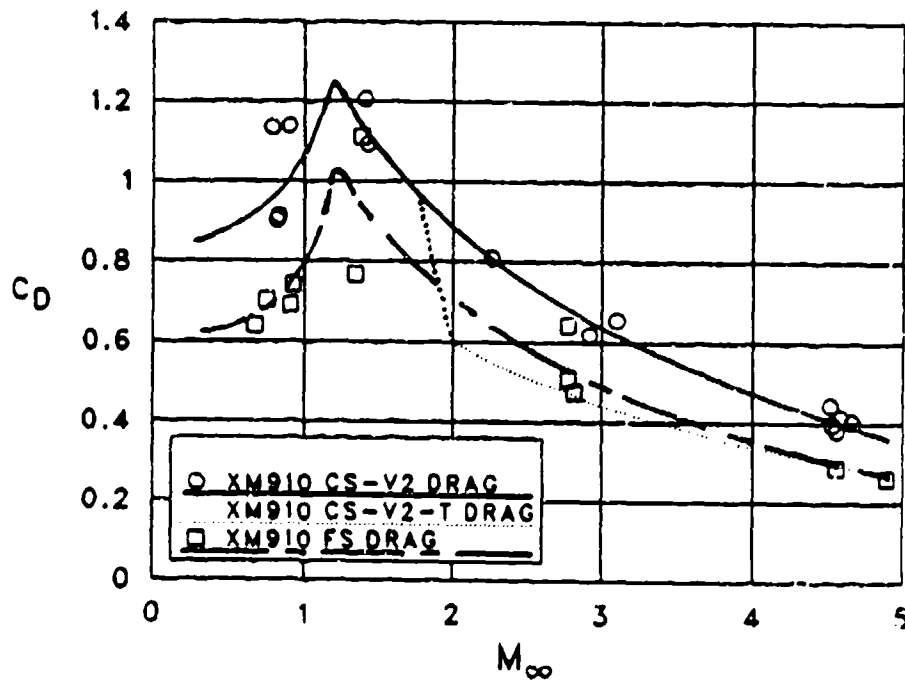
Figure 9. Predicted effect of a tracer on XM910 CS-V2 drag coefficient.
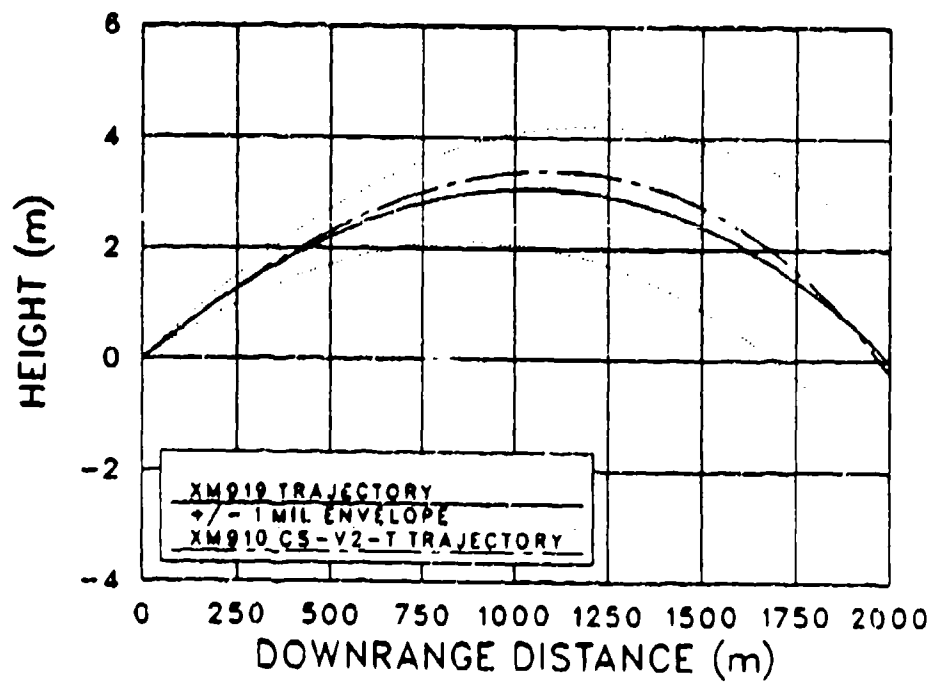
Figure 10. Trajectory comparison of XM910 CS-V2-T with XM919.

16
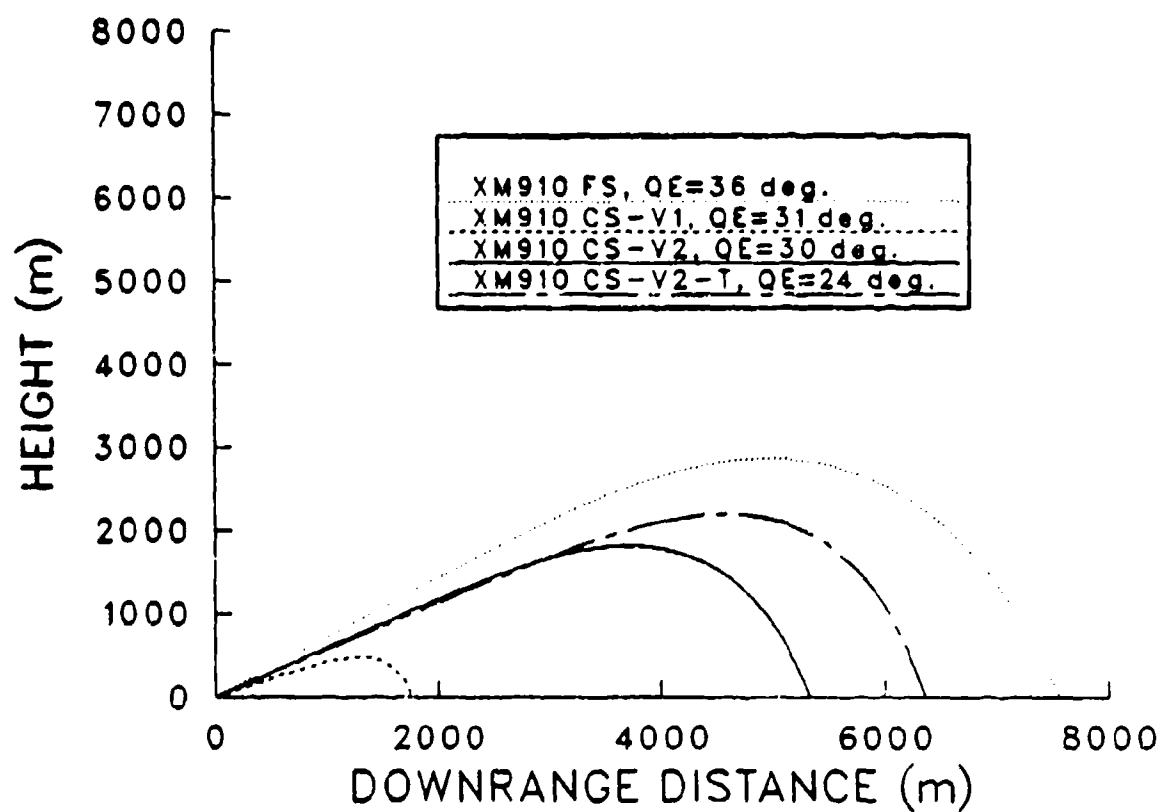
Figure 11. Predicted maximum range trajectories.

17
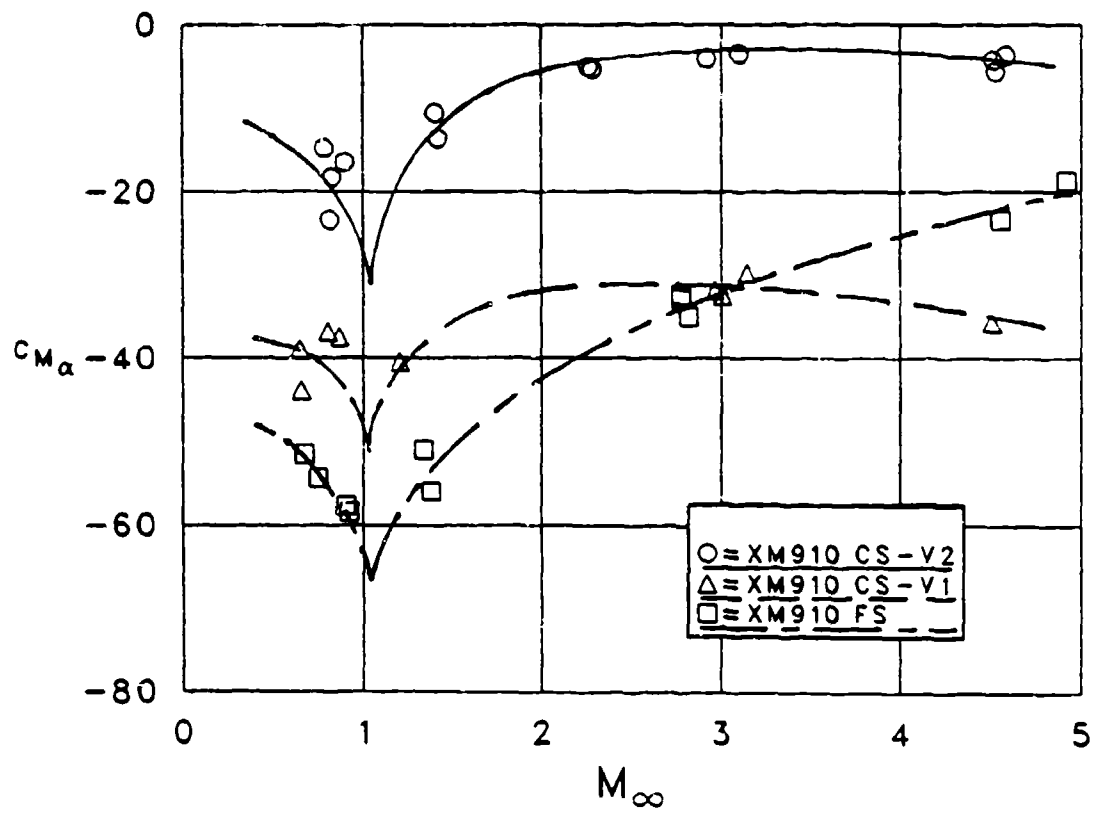
Figure 12. Static moment coefficient versus Mach number.

18
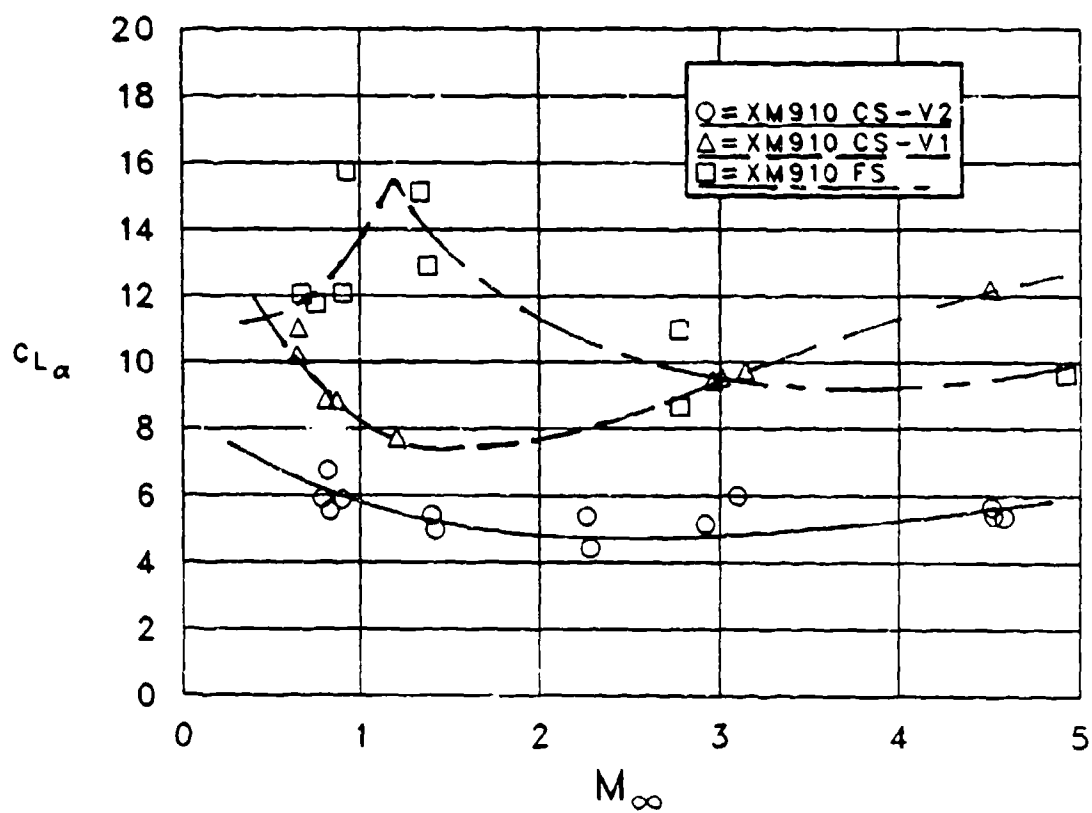
Figure 13. Lift coefficient versus Mach number.

19
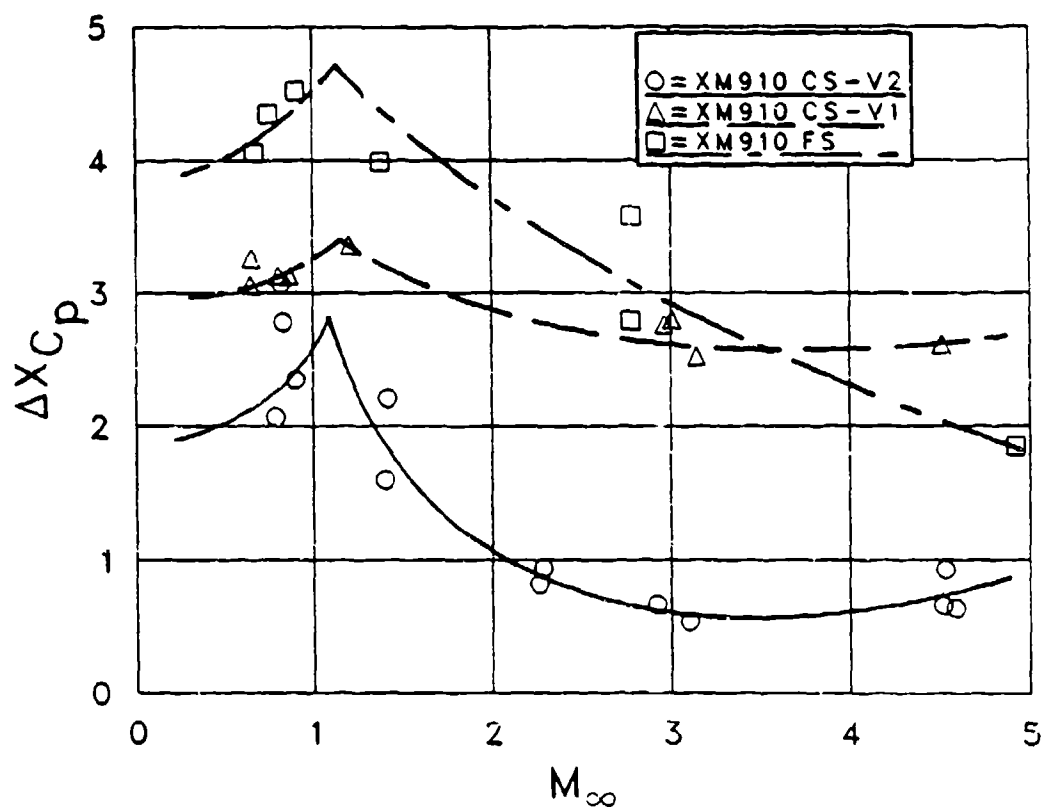
Figure 14. Static margin versus Mach number.

20
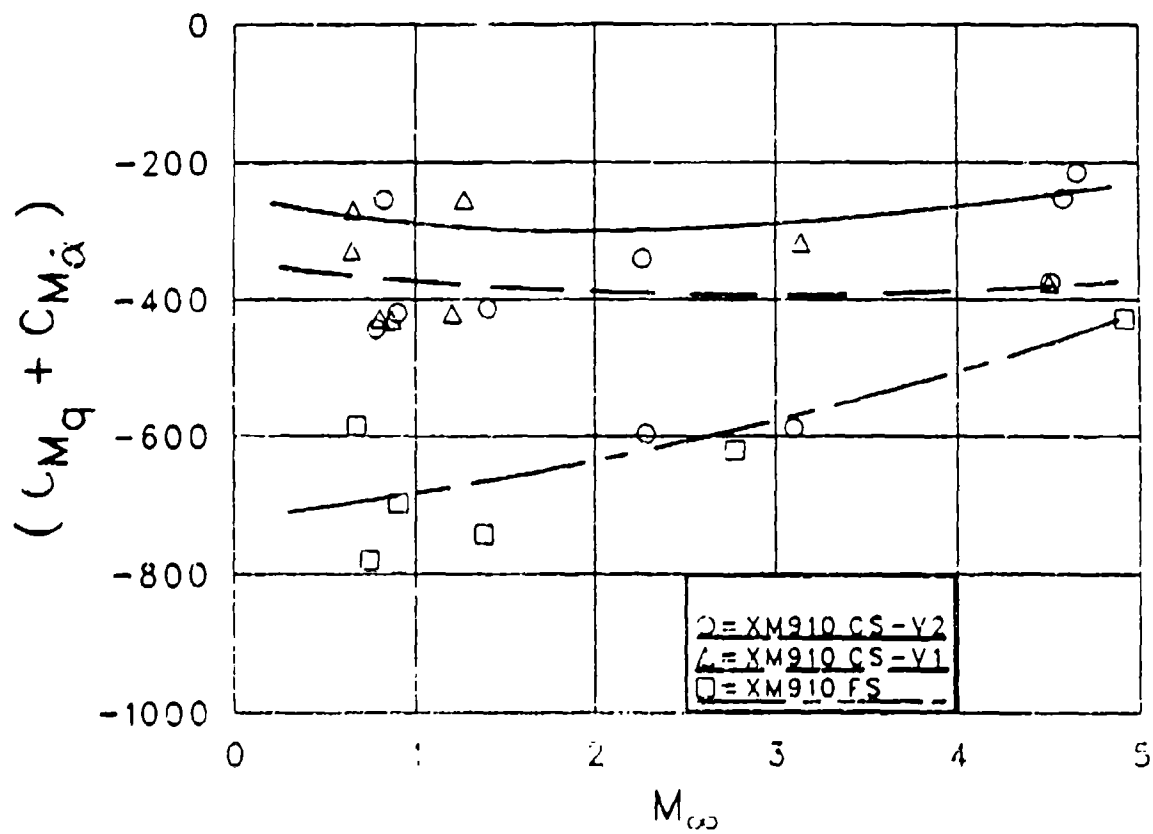
Figure 15. Pitch damping coefficient versus Mach number.

21
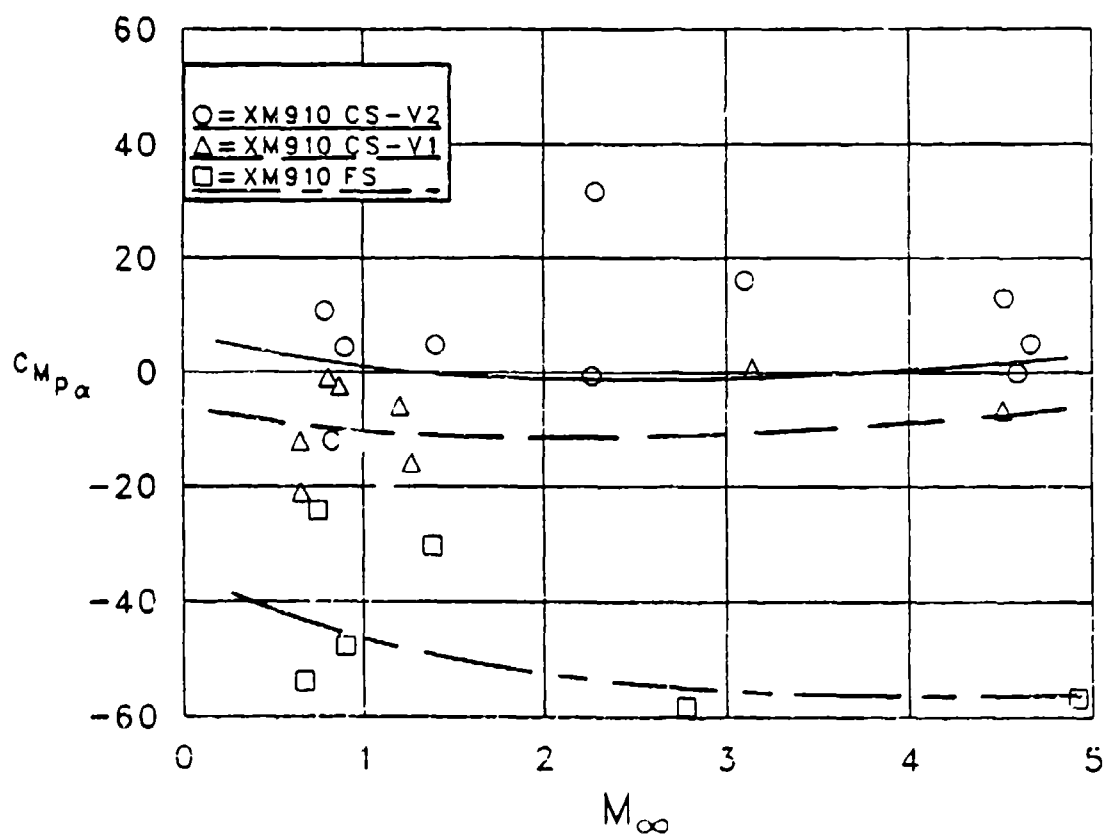
Figure 16. Magnus moment coefficient versus Mach number.

22

REFERENCES

1. Braun, W.F., "The Free Flight Aerodynamics Range," BRL-R-1048, U.S. Army Ballistic Research Laboratory, Aberdeen Proving Ground, Maryland, August 1958. (AD 202249)

2. Murphy, C.H., "Data Reduction for the Free Flight Spark Ranges," BRL-R-900, U.S. Army Ballistic Research Laboratory, Aberdeen Proving Ground, Maryland, February 1954. (AD 35833)

3. Mermagen, W.H., Yalamanchili, R.J., and McElroy, H., "Comparative Flight Tests of Solid and Perforated Flare Stabilized Projectiles," BRL-MR-3540, U.S. Army Ballistic Research Laboratory, Aberdeen Proving Ground, Maryland, August 1986. (AD B10528)

4. Platou, A. J., "The Magnus Force on a Finned Body," BRL-R-1193, U.S. Army Ballistic Research Laboratory, Aberdeen Proving Ground, Maryland, March 1963. (AD 214590)

5. Devan, L., and Mason, L.A., "Aerodynamics of Tactical Weapons to Mach Number 8 and Angle of Attack 180 degrees: Part II, Computer Program and Users Guide," NSWC-TR-81-358, Naval Surface Weapons Center, Dahlgren, Virginia, September 1981. (AD B061071)

6. Vukelich, S.R., "Automated Missile DATCOM: Vol. I - Program User's Guide," McDonnell-Douglas Corporation Report, St. Louis, Missouri, August 1984.

7. McCoy, R.L., "McDrag - A Computer Program for Estimating the Drag Coefficients of Projectiles," ARBRL-TR-02293, U.S. Army Ballistic Research Laboratory, Aberdeen Proving Ground, Maryland, February 1981. (AD A098110)

APPENDIX: DRAG AND STATIC MARGIN ESTIMATES

Test firings of a flare-stabilized projectile (XM910 CS-V1), showed that the drag of this configuration was too high. Thus BRL decided to examine the possibility of designing a flare configuration with low enough drag to meet the training round requirements without losing stability. Several problems had to be resolved before the feasibility of this approach could be determined.

The first problem was to establish the maximum allowable drag for a projectile of this configuration given the training round requirements. This problem was approached by assuming that the basic shape of the drag curve would remain similar to that of the XM910 CS-V1. An iterative approach was then used, where drag curves of varying amplitudes were used as input for trajectory comparisons with the XM919. The resultant maximum drag curve and its corresponding trajectory prediction are shown in Figures A1 and A2, respectively.

The next problem was now to correlate changes in drag and stability with changes in flare geometry. A fast and relatively accurate prediction method was required. Three methods were investigated – a Naval Surface Weapons Center (NSWC) code,[5] the Missile DATCOM Code,[6] and McDrag.[7] All three methods were run using the geometry of the tested 15-degree flare as input, and the predicted drag curves were compared with the measured data. This comparison is shown as Figure A3. As can be seen, the NSWC code yields the best drag prediction, with McDrag as a close second. However, the large variation of the predicted drag curves was somewhat surprising for such a simple projectile shape. A closer examination of the predicted components of axial force showed that the largest variation between methods was in the base pressure drag prediction. This is illustrated by Figure A4, which is a plot of each method's predicted total drag minus the predicted base drag, with the measured total drag included for reference. The consistency of these drag predictions implies that almost all of the variation in total drag is due to differences in estimations of base drag. Furthermore, the difference between the measured total drag and these predictions should be a good measure of the actual base drag, assuming the computed values of forebody drag are correct.

Figure A5 is a plot of the measured and predicted center of pressure (CP) location versus Mach number. Since McDrag does not make this prediction, only the other two codes' results are shown. Again, the NSWC code makes the more accurate prediction. Since the NSWC code was found to be most accurate for both drag and CP location, it was chosen to be used for the analysis.

Now that the required drag was known and a predictive method was available, the next problem was to determine exactly how the flare length, flare angle, drag, and stability are related. This was done using a two-part parametric analysis. First, the NSWC code was run for all possible combinations of flare half-angles of 5.0, 7.5, 10.0, 12.5, and 15.0 degrees, with flare lengths of 0.5, 1.0, 1.5, 2.0, 2.5, and 3.0 calibers. The projectile forebody configuration was kept constant in each case. The predicted total drag was then plotted at Mach numbers of 4, 3 and 2, the lower number being the expected velocity at 2000 meters. These plots are presented as Figures A6a, A6b, and A6c, respectively. Also shown on these plots is a horizontal line at the maximum allowable drag, calculated earlier. These graphs were then used

to determine the maximum length for each flare angle that would meet the drag criteria. Figure A7 shows the relative sizes of these low-drag flares, with the tested configuration included for comparison. With the exception of this tested configuration, all of the rounds in the figure have essentially the same drag, even though the flare shapes are radically different.

For the second part of the analysis, the qualifying configurations were analyzed for stability. The center of gravity (CG) location of each projectile was calculated, based on the projectile geometry and material densities. The NSWC code was then run for each of the low-drag flare geometries, and the CP location was predicted. The distance of the CP behind the CG (static margin) was plotted against Mach number for each low-drag shape, included as Figure A8. Theoretically, a round of this type is statically stable if the static margin is positive. However, experience has shown that a more realistic criterion for stability is to have a static margin of at least 0.5. Examination of Figure A8 shows that only the 5-degree flare configuration is predicted to be stable by this method, and only marginally so. Taking into account the fact that the NSWC code seems to overpredict the static margin (see Figure A5), the stability of this flare becomes even more questionable. However, Figure A8 also shows a distinct trend: for a given drag, longer, smaller angle flares are more stable. Based on this trend, it was decided to examine the effects of using smaller flare angles.

The entire analysis was then repeated for flare half-angles of 2, 3, and 4 degrees. Figure A9 shows the resultant static margins, including the 5 degree flare. The relative sizes of all the stable, low drag flares are depicted by Figure A10. The 4-degree configuration was ultimately chosen for further testing because it was the shortest flare predicted to remain stable down to Mach 2. Additionally, the length and weight of this flare were almost identical to those of the standard fins. The 2- and 3-degree flares were predicted to have better static stability, but these flares were suspected of being structurally unsound because of their extreme length. A series of test firings of the 4-degree flare design was then conducted. Figure A11 shows the drag predicted by each of the three methods mentioned previously, compared with the measured drag. Figure A12 again shows the predicted values without base drag, displaying the same pattern discussed earlier. Finally, Figure A13 compares the measured and predicted static margin.
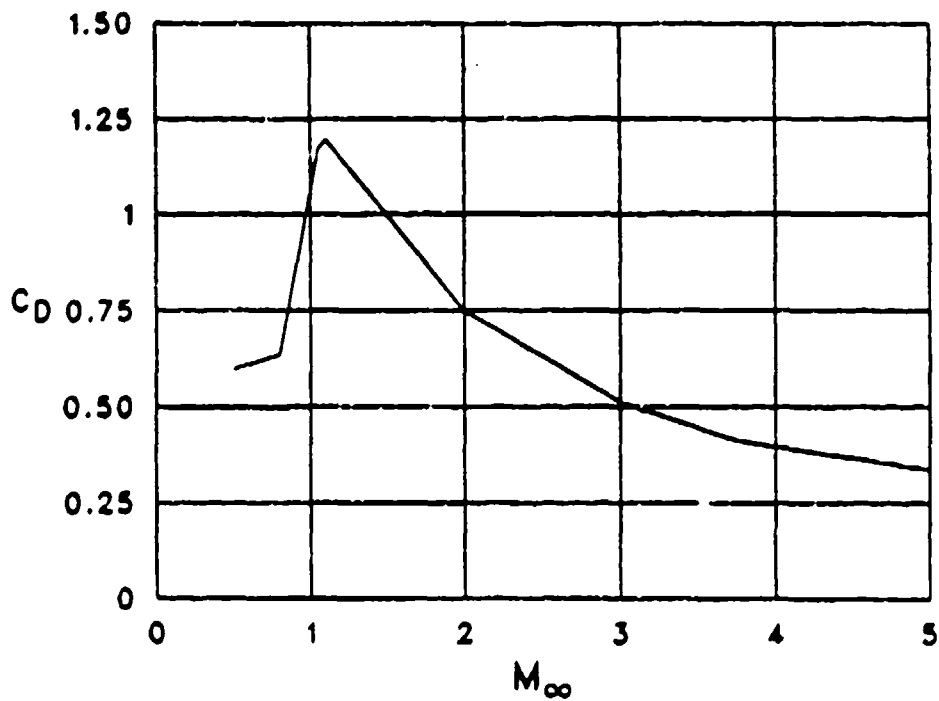
Figure A-1. Maximum XM910 drag that will fulfill ballistic requirements.
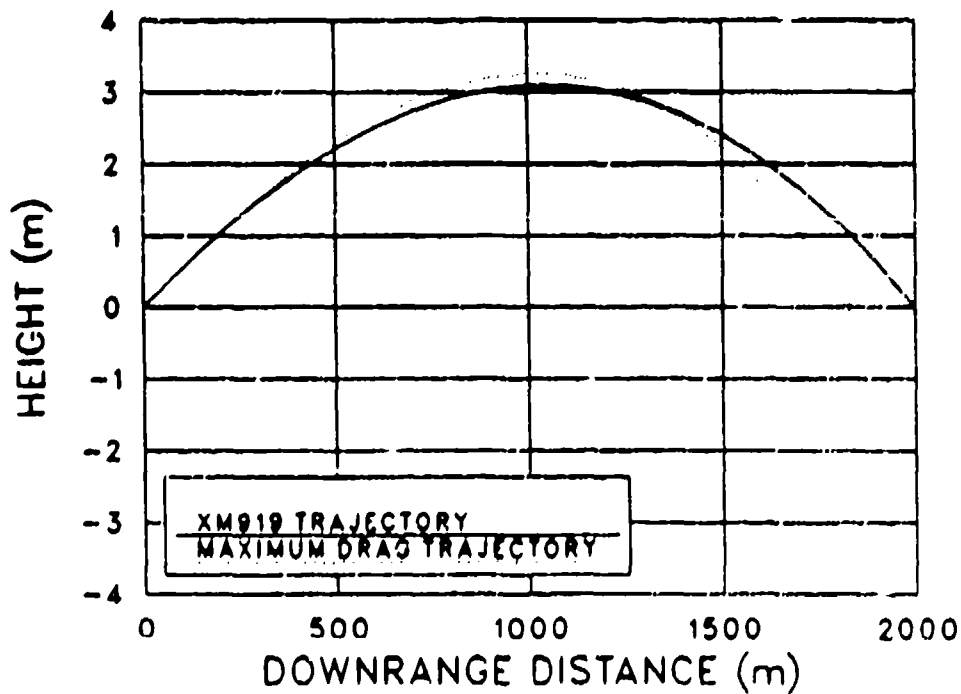

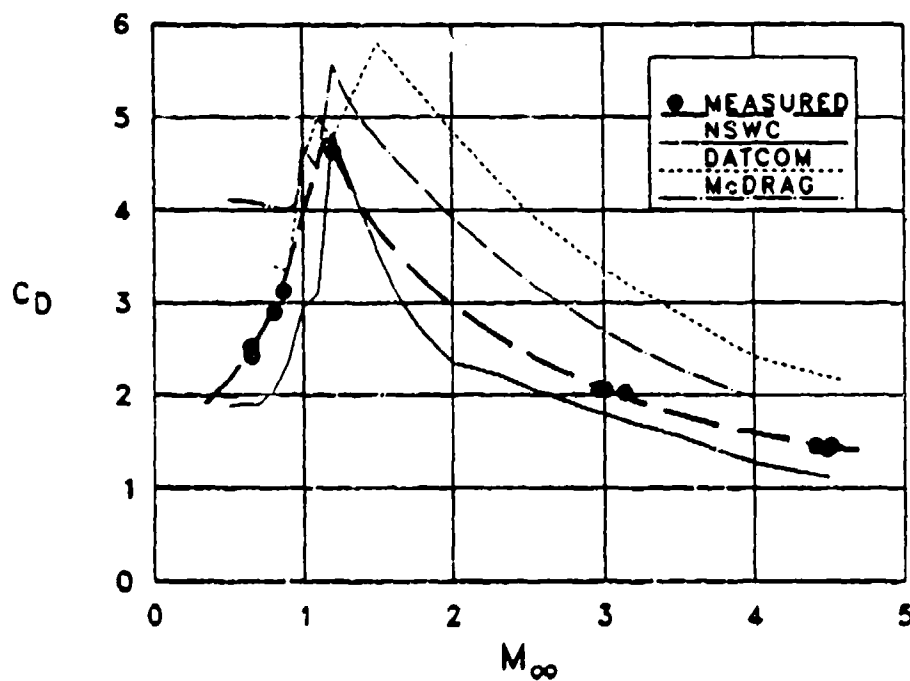Figure A-2. Trajectory comparison of maximum drag XM910 with XM919.

27

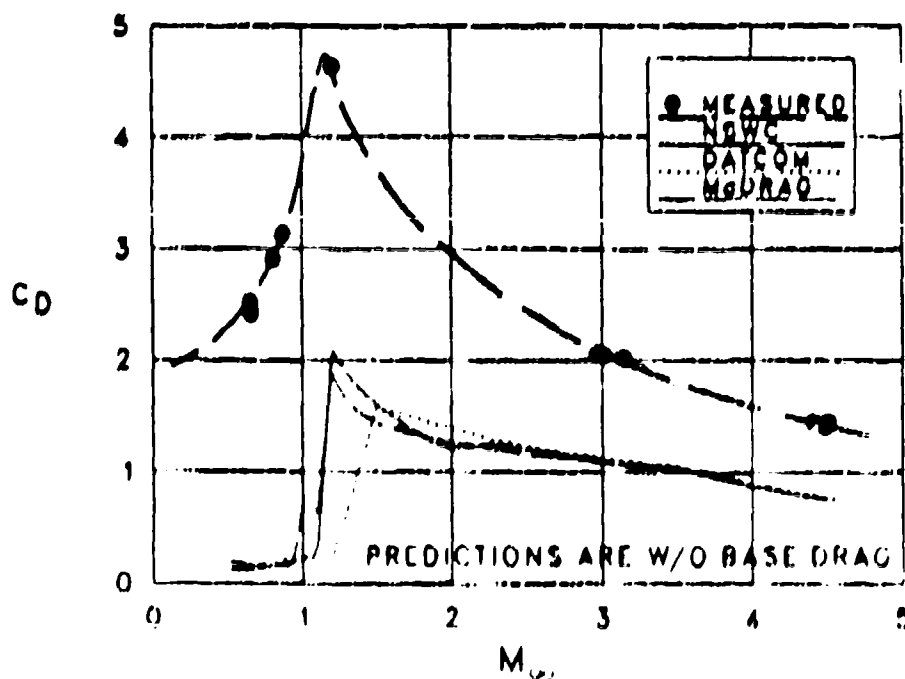**Figure A-3.** Measured and predicted drag coefficient versus Mach number, XM910 CS-V1.

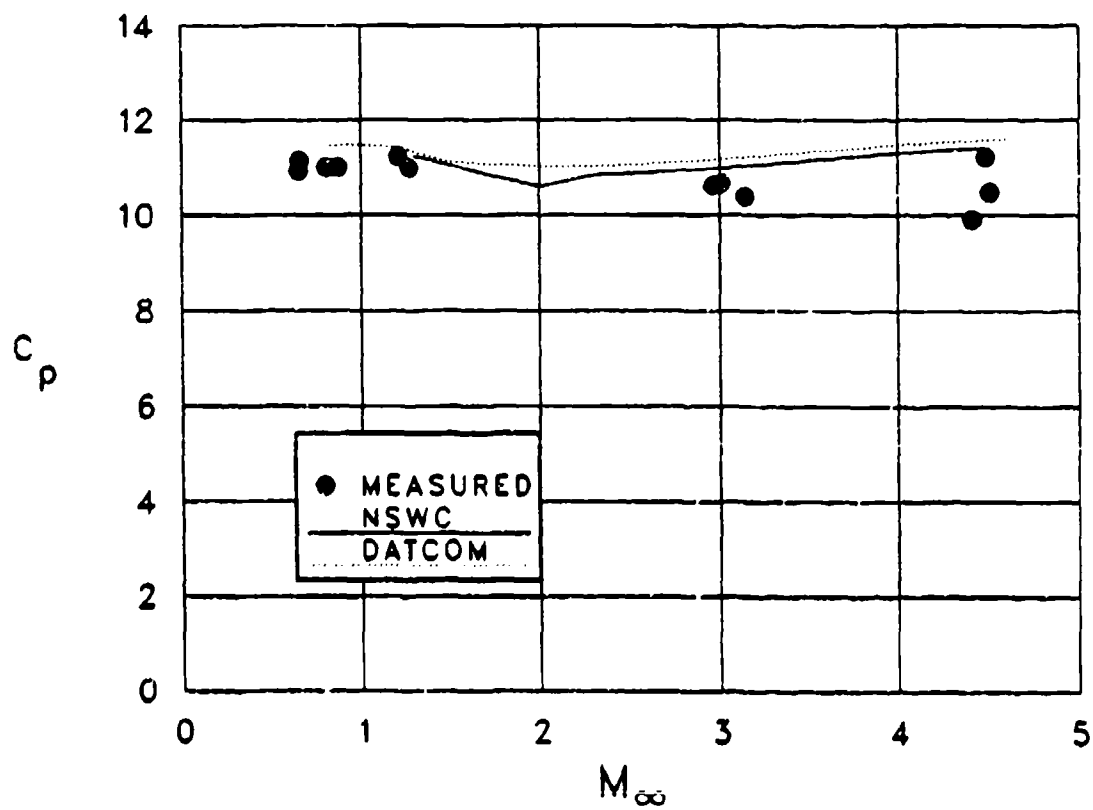**Figure A-4.** Comparison of measured drag and predicted drag without base drag, XM910 CS-V1.

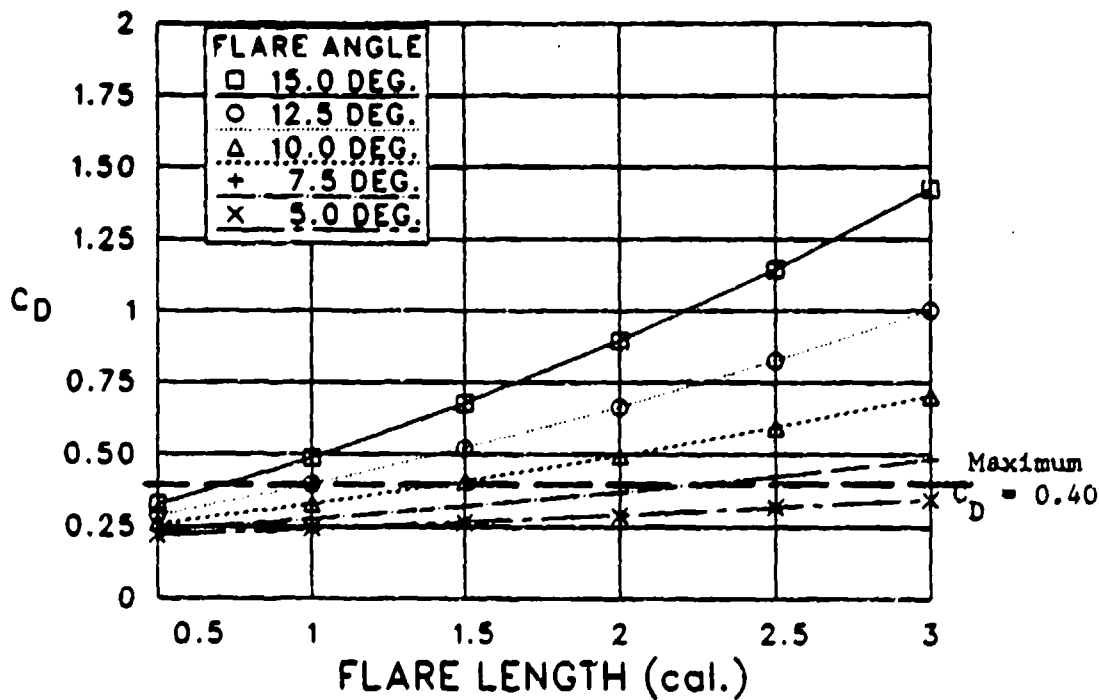Figure A-5. Measured and predicted center of pressure location (calibers from nose) versus Mach number, XM910 CS-V1.

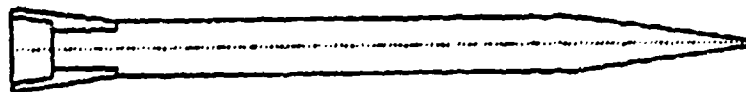Figure A-6a. Predicted drag coefficient versus flare length (calibers) at Mach 4.
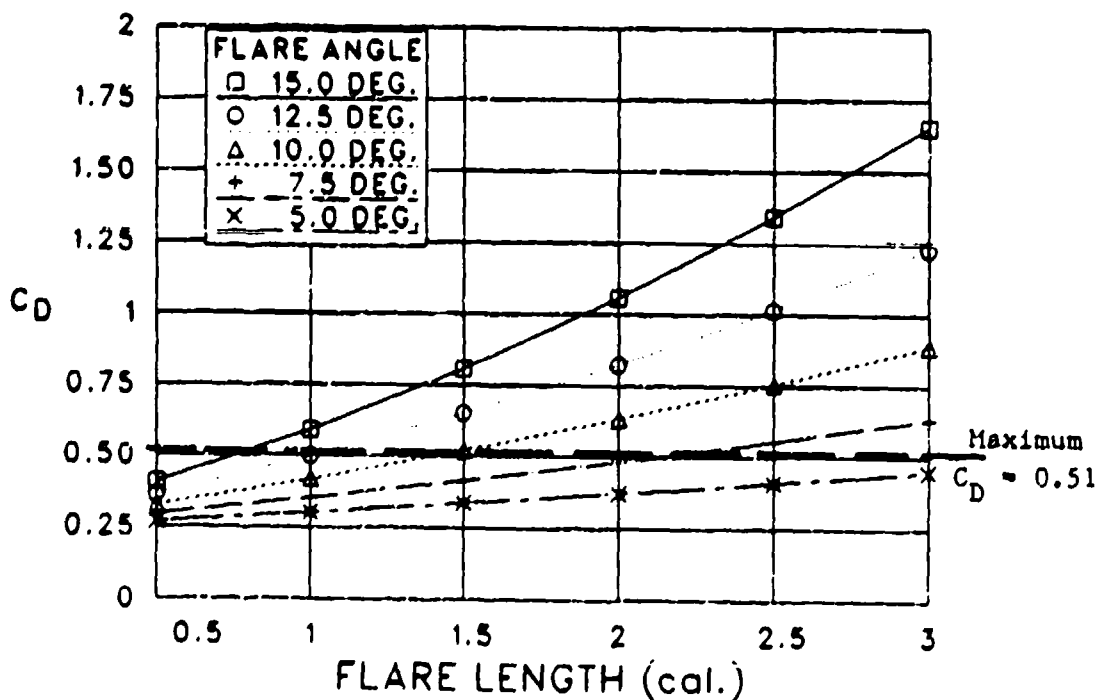
Figure A-6b. Predicted drag coefficient versus flare length (calibers) at Mach 3.
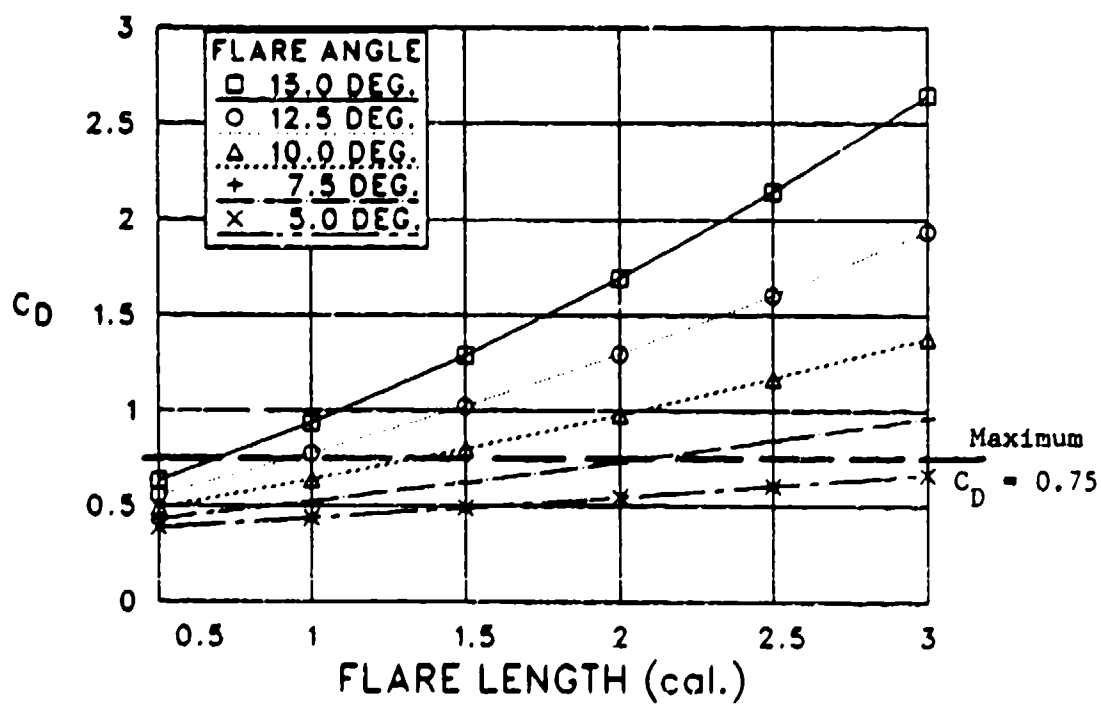
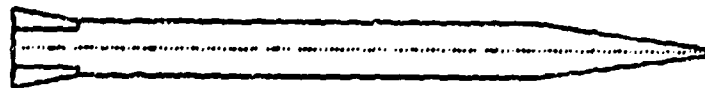Figure A-6c. Predicted drag coefficient versus flare length (calibers) at Mach 2.
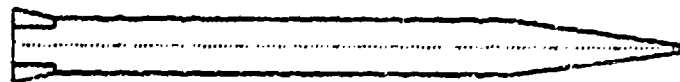
5.0 deg., 3.5 cal.
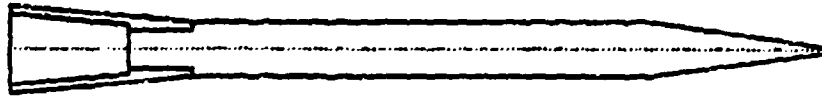
7.5 deg., 2.0 cal.

10.0 deg., 1.25 cal.

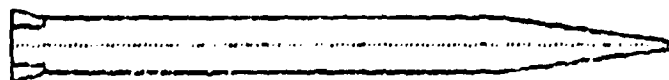12.5 deg., 0.8 cal.

15.0 deg., 0.6 cal.

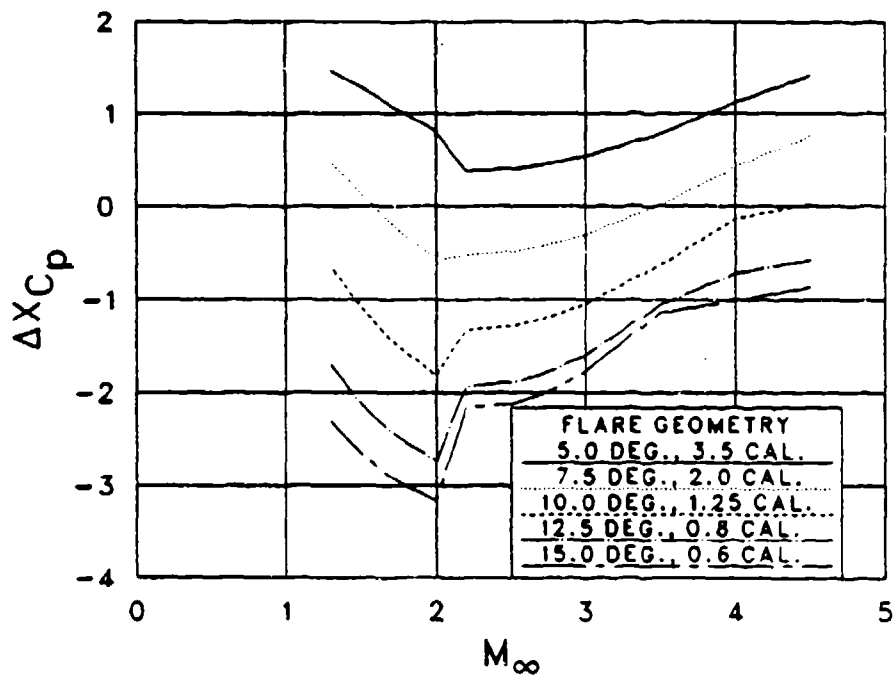Figure A-7. Low drag flare configurations.
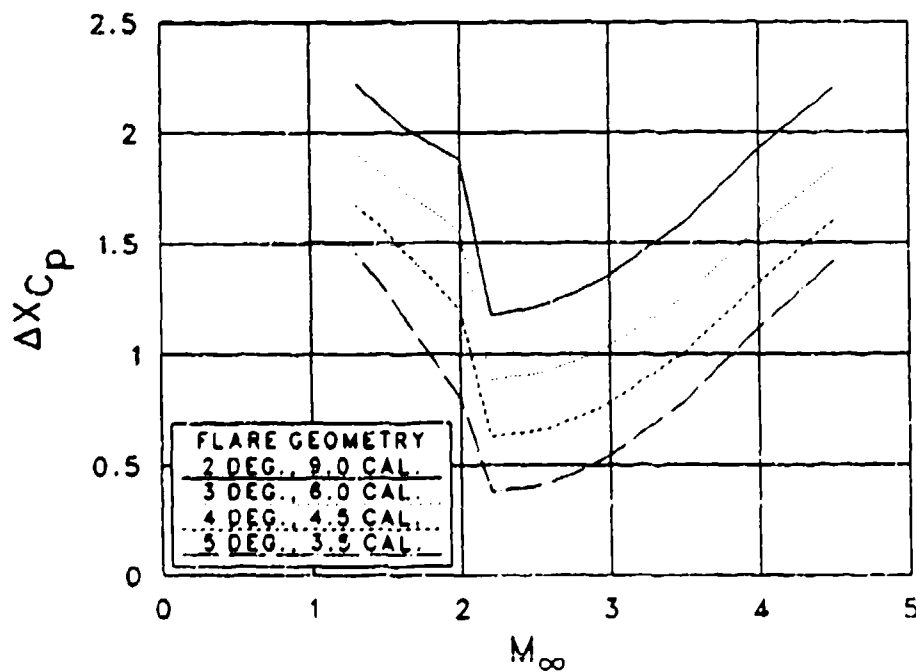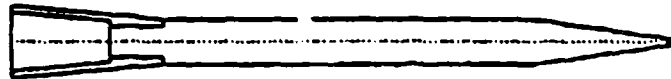
Figure A-8. Static margin versus Mach number.

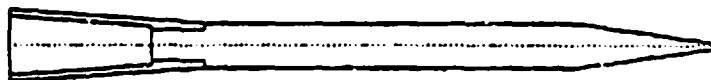Figure A-9. Static margin versus Mach number, small flare angles.
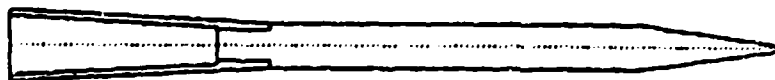
5.0 deg., 3.5 cal.

4.0 deg., 4.5 cal.

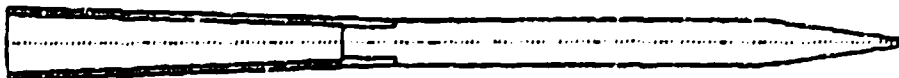# 3.0 deg., 6.0 cal.

2.0 deg., 9.0 cal.

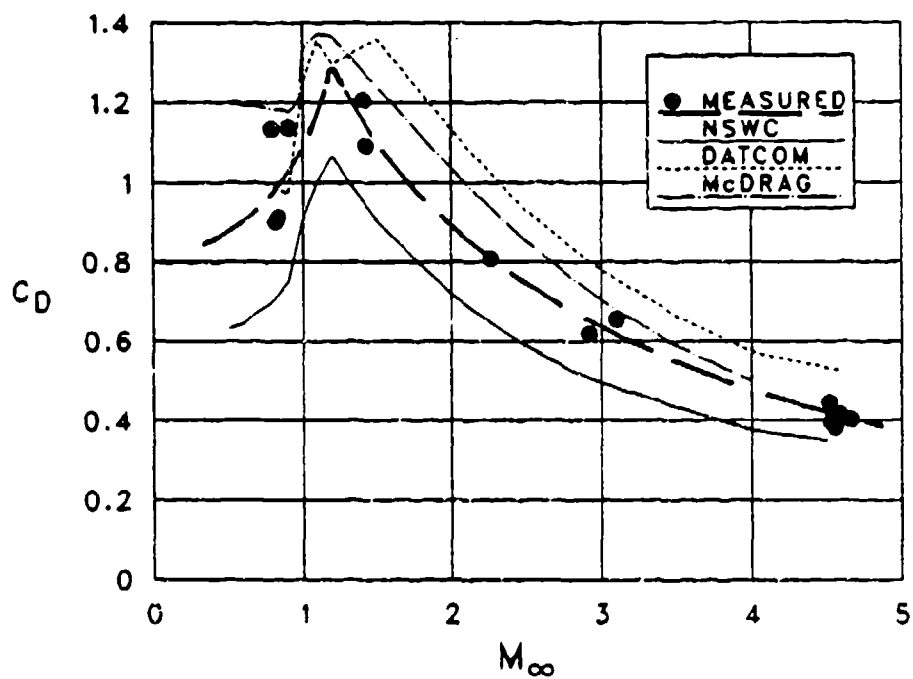Figure A-10.   Stable low drag flare configurations.

Figure A-11. Measured and predicted drag coefficient versus Mach number, XM910 CS-V2.
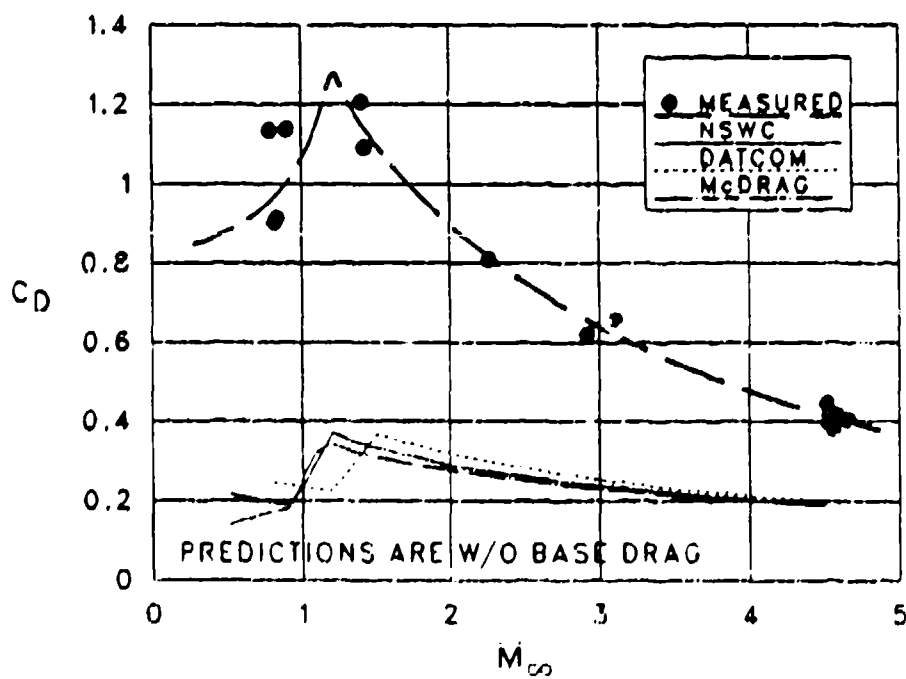

Figure A-12. Comparison of measured drag and predicted drag without base drag, XM910 CS-V2.
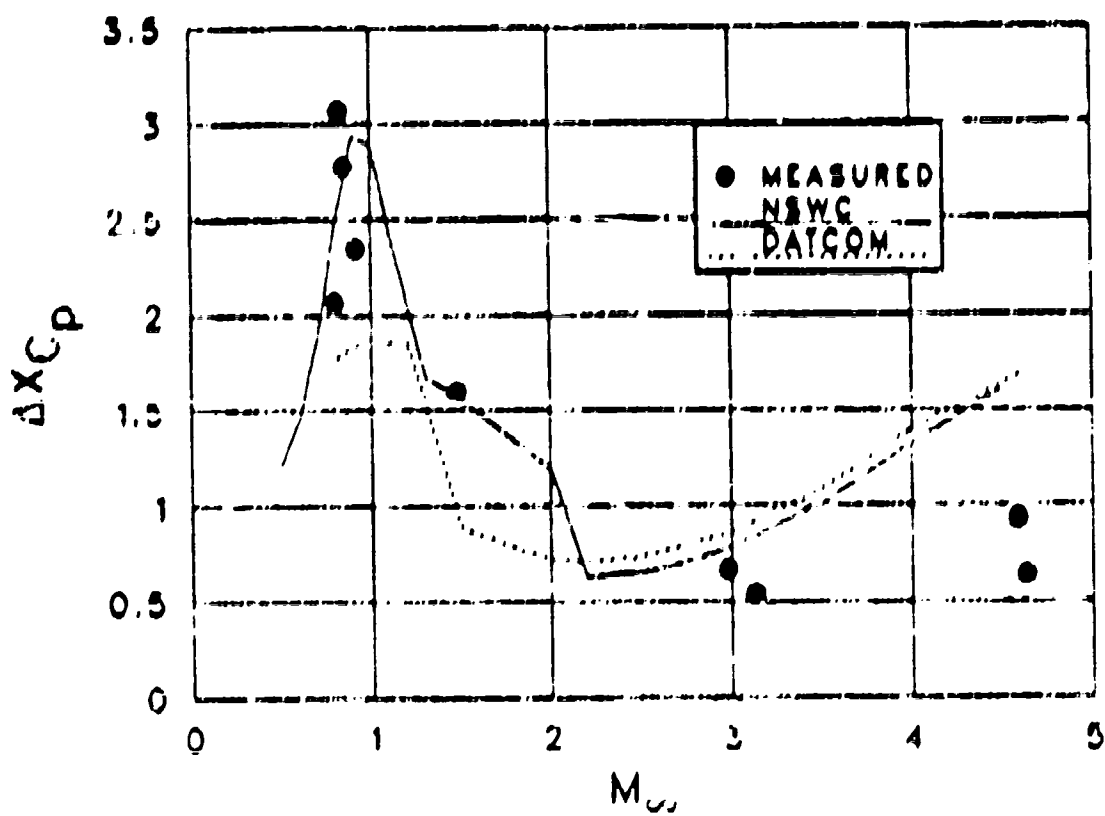
Figure A-13. Measured and predicted static margin, XM920-V2.

DISTRIBUTION LIST

No. of Copies	Organization	No. of Copies	Organization
12	Administrator Defense Technical Info Center ATTN: DTIC-FDAC Cameron Station, Bldg. 5 Alexandria, VA 22304-6145	1	Commander US Army Tank Automotive Command ATTN: AMSTA-TSL Warren, MI 48397-5000
1	HQDA DAMA-ART-M Washington, DC 20310	1	Commander US Army Armament Munitions & Chemical Command ATTN: AMSMC-IMP-L Rock Island, IL 61299-7300
1	Commander US Army Materiel Command ATTN: AMCDRA-ST 5001 Eisenhower Avenue Alexandria, VA 22333-0001	8	Commander Armament RD&E Center US Army AMCCOM ATTN: SMCAR-MSI SMCAR-CCL-CA, Peter O'Neill Carol Ann Miller E. Malatesta
1	Director US Army Aviation Research and Technology Activity Ames Research Center Moffett Field, CA 94035-1099		R. Cickora J. Hirlinger ATTN: SMCAR-AET-A, G. Fleming Dover, NJ 07801-5001
1	Commander US Army Communications - Electronics Command ATTN: AMSEL-ED Fort Monmouth, NJ 07703-5301	1	Commander Armament RD&E Center US Army AMCCOM ATTN: SMCAR-TDC Dover, NJ 07801-5001
1	Commander CECOM R&D Technical Library ATTN: AMSEL-IM-L (Reports Section) B.2700 Fort Monmouth, NJ 07703-5000	1	Commander U.S. AMCCOM ARDEC CCAC Benet Weapons Laboratory ATTN: SMCAR-CCB-TL Watervliet, NY 12189-4050
1	Commander U.S. Army Missile Command Research, Development, and Engineering Center ATTN: AMSMI-RD Redstone Arsenal, AL 35898-5230	1	Commandant US Army Infantry School ATTN: ATSH-CD-CS-OR Ft. Benning, GA 31905-5400
1	Commander US Army Missile and Space Intelligence Center ATTN: AIAMS-YDL Redstone Arsenal, AL 35898-5000	1	Commander US Army Development and Employment Agency ATTN: MODE-ORO Fort Lewis, WA 98433-5000

DISTRIBUTION LIST (continued)

No. of Copies	Organization
1	Director US Army TRADOC Analysis Center ATTN: ATOR-TSL White Sands Missile Range, NM 88002-5502
1	AFWL/SUL Kirtland AFB, NM 87117
1	Air Force Armament Laboratory ATTN: AFATL/DLODL (Tech Info Center) Eglin AFB, FL 32542-5000
10	C.I.A. OIR/DB/Standard GE47 HQ Washington, D.C. 20505
1	Commander US Army Aviation Systems Command ATTN: AMSAV-ES 4300 Goodfellow Blvd St. Louis, MO 63120-1798
1	AFELM, The Rand Corporation ATTN: Library-D 1700 Main Street Santa Monica, CA 90406

4	Ford Aerospace & Communications
	        Corporation
	Ford Road
	ATTN: Charles O. White
	          Bud Blair
	          Ken Zeroll
	          Chuck Rippe
	Newport Beach, CA 92660

2	Honeywell, Inc. 600 Second Street, NE ATTN: W.E. Martwick Ken Sundeen Hopkins, MN 55343

No. of Copies	Organization

5	Aerojet Ordnance Company
	Tustin Facility
	ATTN: Jim Parkinson
	          Doug LaFevre
	          Saul Wasserman
	          Abe Flatou
	          S.K. Rush
	2521 Michelle Drive
	Tustin, California 92680

Aberdeen Proving Ground

Dir, USAMSAA
ATTN: AMXSY-D
          AMXSY-MP, H. Cohen

Cdr, USATECOM
ATTN: AMSTE-SI-F

Cdr, CRDEC, AMCCOM
ATTN: SMCCR-RSP-A
          SMCCR-MU
          SMCCR-SPS-IL

38

USER EVALUATION SHEET/CHANGE OF ADDRESS

This Laboratory undertakes a continuing effort to improve the quality of the reports it publishes. Your comments/answers to the items/questions below will aid us in our efforts.

1. SRL Report Number_____Date of Report_____

2. Date Report Received_____

3. Does this report satisfy a need? (Comment on purpose, related project, or other area of interest for which the report will be used.)_____

_____

_____

4. How specifically, is the report being used? (Information source, design data, procedure, source of ideas, etc.)_____

_____

_____

5. Has the information in this report led to any quantitative savings as far as man-hours or dollars saved, operating costs avoided or efficiencies achieved, etc? If so, please elaborate._____

_____

_____

6. General Comments. What do you think should be changed to improve future reports? (Indicate changes to organization, technical content, format, etc.)

_____

_____

_____

	Name_____
CURRENT ADDRESS	Organization_____
	Address_____
	City, State, Zip_____

7. If indicating a Change of Address or Address Correction, please provide the New or Correct Address in Block 6 above and the Old or Incorrect address below.

	Name_____
OLD ADDRESS	Organization_____
	Address_____
	City, State, Zip_____

(Remove this sheet, fold as indicated, staple or tape closed, and mail.)